Annals of Biomedical Engineering (© 2013)
DOI: 10.1007/s10439-013-0923-2

BMES BIOMEDICAL ENGINEERING SOCIETY™ www.bmes.org

In Vitro and Numerical Support for Combinatorial Irreversible Electroporation and Electrochemotherapy Glioma Treatment

R. E. Neal II,[1,2] J. H. Rossmeisl Jr.,[3] V. D'Alfonso,[3] J. L. Robertson,[4] P. A. Garcia,[1] S. Elankumaran,[5] and R. V. Davalos[1]

[1]Bioelectromechanical Systems Lab, Virginia Tech – Wake Forest School of Biomedical Engineering and Sciences, Blacksburg, VA, USA; [2]Radiology Research Unit, The Alfred Hospital, 55 Commercial Road, Melbourne, VIC 3004, Australia; [3]Neurology/Neurosurgery Service and Center for Comparative Oncology, VA-MD Regional College of Veterinary Medicine, Blacksburg, VA, USA; [4]Cancer Engineering Group, Virginia Tech – Wake Forest School of Biomedical Engineering and Sciences, Blacksburg, VA, USA; and [5]Department of Biomedical Sciences and Pathobiology, VA-MD Regional College of Veterinary Medicine, Blacksburg, VA, USA

(*Received 12 April 2013; accepted 4 October 2013*)

Associate Editor Agata A. Exner oversaw the review of this article.

Abstract—Irreversible electroporation (IRE) achieves targeted volume non-thermal focal ablation using a series of brief electric pulses to kill cells by disrupting membrane integrity. Electrochemotherapy (ECT) uses lower numbers of sub-lethal electric pulses to disrupt membranes for improved drug uptake. Malignant glioma (MG) brain tumors are difficult to treat due to diffuse peripheral margins into healthy neural tissue. Here, *in vitro* experimental data and numerical simulations investigate the feasibility for IRE-relevant pulse protocols with adjuvant ECT drugs to enhance MG treatment. Cytotoxicity curves were produced on two glioma cell lines *in vitro* at multiple pulse strengths and drug doses with Bleomycin or Carboplatin. Pulses alone increased cytotoxicity with higher pulse numbers and strengths, reaching >90% by 800 V/cm with 90 pulses. Chemotherapeutic addition increased cytotoxicity by >50% for 1 ng/mL concentrations of either drug relative to 80 pulses alone with J3T cells at electric fields ≥400 V/cm. In addition to necrosis, transmission electron microscopy visualizes apoptotic morphological changes and Hoescht 33342 staining shows apoptotic cell fractions varying with electric field and drug dose relative to controls. Numerically simulated treatment volumes in a canine brain show IRE combined with ECT expands therapeutic volume by 2.1–3.2 times compared to IRE alone.

Keywords—Combined therapy, Non-thermal focal ablation, Brain cancer, IRE, ECT, Numerical modeling, Minimally invasive surgery, Multimodality oncology, Targeted therapy.

Address correspondence to R. E. Neal II, Radiology Research Unit, The Alfred Hospital, 55 Commercial Road, Melbourne, VIC 3004, Australia. Electronic mail: robert.neal@alfred.org.au

R.E. Neal II and J.H. Rossmeisl Jr. have contributed equally to this work.

ABBREVIATIONS

IRE	Irreversible electroporation
ECT	Electrochemotherapy
BBB	Blood–brain-barrier

INTRODUCTION

Therapeutic options for brain and central nervous system malignancies include radiation therapy, surgical resection, chemotherapeutics, or a combination of these modalities.[29] Despite their availability, only 7 months have been added to the mean malignant glioma (MG) patient survival in the past 70 years.[24] One poor survival cause is that glioma cells infiltrate up to 2 cm beyond visible tumor margins.[17] In addition, the blood–brain-barrier (BBB) and an inherent resistance of glioma cells to conventional drug therapies diminishes MG treatment outcomes.[14]

Focal ablation therapies provide advantageous low morbidity alternatives to surgical intervention.[2] Such approaches include thermally based cell death mechanisms, such as cryoablation and radiofrequency ablation; and non-thermal pathways, including percutaneous ethanol injection and irreversible electroporation (IRE). IRE is a non-thermal focal ablation tumor treatment technique,[3,27,37] including MGs.[11] It uses electric pulses delivered through needle electrodes placed within the targeted region to kill cells by disrupting cellular membrane integrity.[8] IRE achieves cell death non-thermally; sparing the extracellular matrix and sensitive structures such as the major vasculature,

Published online: 29 October 2013

thus permitting treatment in regions unsuitable for surgical resection or thermal therapies.[8,28] Treatments facilitate rapid lesion creation and resolution, are unaffected by blood perfusion effects, and may be monitored in real-time.[25] There is a sharp demarcation between treated and normal regions[8] based on the electric field distribution, permitting numerical simulations treatment planning.[22]

Limitations for focal therapies include their locoregional nature and success being correlated with tumor size; likely due to the complexity of overlapping ablation zones required for complete coverage of the targeted lesion and margin.[38] This has led investigators to combine focal ablation with adjuvants such as chemotherapeutics, anti-angiogenics, and immunostimulants; achieving improved patient survival and experimental distant tumor responses.[2,30,31,33] Similar efficacy constraints exist for IRE regarding lesion size and systemic infiltration,[5] suggesting IRE will also benefit from combinatorial approaches.

Electrochemotherapy (ECT) uses chemotherapeutics with reversible electroporation, where cells survive pore formation by avoiding the irreversible regime of the electric pulse protocols.[23] ECT uses intravenous or intratumoral chemotherapeutics with poor natural cellular infiltration, then delivers a short series of pulsed electric fields to reversibly electroporate cells in a targeted region, locally enhancing cellular uptake and toxicity by several orders of magnitude.[23] Because the drugs used can target rapidly dividing cells, they exhibit some selective ability.[23]

ECT is becoming common in the management of small cutaneous tumors,[15] and is beginning to be used for deep-seated tumors. Where ECT therapies avoid the IRE realm, they utilize a distinct set of pulse parameters, with protocols of 8–12 pulses to generate the largest enhancement of drug cytotoxicity without innately killing the cells,[36] much fewer than IRE (≥80).[37] This gives ECT a narrower functional bandwidth of pulse protocols, limiting the size of effective treatment zones where destruction of all cancerous cells can be assured.

IRE reliably kills all cells within the ablation margins with discrete boundary demarcation, which is typically unselective. IRE has a large bandwidth of treatment parameters to kill cells, making it well suited for destroying the entire visible tumor; while infiltrative cells beyond this region may be selectively targeted with chemotherapeutics in the sub-lethal electric field realms beyond the IRE margin. Combining IRE primary tumor control with the inclusion of adjuvants that exploit the sub-lethal electric field has been previously suggested,[6] and has been shown for gene therapy,[4] but has not been extensively examined for drug delivery. This may be due to the distinct optimal electric pulse parameters between ECT-explicit and IRE-alone therapies.

In our study, we provide *in vitro* evidence supporting potential therapeutic response enhancement in MGs by combining IRE protocols with common ECT chemotherapeutics to synergistically expand therapeutic margins beyond the initial IRE zone, ideally targeting infiltrative neoplastic cells among healthy tissue. To evaluate a synergistic effect, it must be determined if enhanced chemotherapeutic cytotoxicity exists at sub-lethal electric fields when employing clinical IRE pulse protocols. This is important because increasing the number of pulses decreases the lethal electric field threshold.[32] Therefore, the higher IRE pulse number protocols may eliminate the realm of permeabilized cells that survive the pulses. The concern addressed here is if the increased number of pulses kills all of the permeabilized cells, leaving no surviving electroporated cells to take in the ECT drug to expand the therapeutic margin.

MGs are well suited for combinatorial IRE with ECT due to the infiltrative nature of MG cells and the need to preserve healthy brain tissue. One major chemotherapy limitation for MGs is the BBB, shielding the tumors from drugs in the bloodstream. The reversible and irreversible disruption of cellular membrane integrity likely bypasses the vessel endothelial and glial cell protective mechanisms that comprise the BBB. This is supported by evidence suggesting BBB disruption in electroporated regions,[13,16,34] allowing otherwise impermeable molecules access to electroporated interstitial spaces. This makes an electroporation-oriented approach to MGs ideal. In rat brain tumors, a 69% regression rate using ECT alone was achieved *in vivo*,[1] and a human clinical trial using ECT as the sole therapy for brain metastases has begun.[20]

This study examines the presence of a persistent cooperative effect between IRE and ECT by developing dose–response curves for two MG cell lines. Cells were exposed to a range of electric pulses and doses of Bleomycin and Carboplatin, two common ECT drugs due to their neoplastic cell selectivity and inherently increased cytotoxicity from electroporation.[23] Sub-lethal electric fields found to synergistically increase cytotoxicity were incorporated into a numerical simulation to predict the regions of IRE ablation and margins for enhanced drug cytotoxicity.

MATERIALS AND METHODS

In Vitro Characterization of Cellular Response

Glioma Cell Lines and Cultures

Canine J3T glioma cells and human U-87 MG (ATCC, Rockville, MD) cell lines were cultured in 75 cm^2 flasks in RPMI1640 medium (Cellgro, Mediatech, Manassas, VA) with supplemental 10% fetal

bovine serum (Atlanta Biologicals, Lawrenceville, GA) and 5% anti-biotic/mycotic solution (Cellgro) in a 5% CO_2 chamber at 37 °C. The canine J3T line was originally obtained from Dr. Michael Berens, Catholic Health Care West, AZ.

Cells were detached using trypsin–EDTA (0.05% trypsin–0.5 mM EDTA; Cellgro), and collected by centrifugation. Cells were washed three times in a low conductivity buffer composed of a 3:1 ratio of RPMI1640 media combined with a buffer solution composed of 85 g sucrose, 3 g glucose, and 7.25 mL RPMI1640 (all from Fisher Scientific, Pittsburgh, PA) blended in 992.75 mL deionized water. Cells were then resuspended in the buffer and counted using a Cellometer (Nexelcom, Lawrence, MA). All experiments used suspensions with >95% viability.

Chemotherapeutic Agent Preparation

Based on results of the growth inhibition assays, six concentrations of Bleomycin (0 pg/mL, 1 pg/mL, 100 pg/mL, 10 ng/mL, 1, and 100 μg/mL) and seven concentrations of Carboplatin (1 mg/mL in addition to the concentrations for Bleomycin) were evaluated. For each drug, concentration, and cell line: mixtures of 2×10^6 cells/mL and each drug at the appropriate concentration (RPMI1640 alone for IRE-only) were placed into 6 individual, 4 mm gap electroporation cuvettes (BTX Cuvette Plus 640, Harvard Apparatus, Holliston, MA) and incubated at room temperature for 10 min prior to IRE pulsing as described below.

Chemotherapeutic Agent Cell Growth Inhibition

Baseline chemotherapeutic cytotoxicity was determined for Bleomycin (Hospira, Lake Forest, IL) and Carboplatin (Sigma, St. Louis, MO) with crystal violet assay. Cytotoxicity against J3T and U-87 MG cells was measured using serial two-fold dilutions of each agent in 96-well plates in triplicate, and then adding 2×10^3 J3T or U-87 MG cells to each well, with a final volume of 100 μL. Initial Bleomycin concentration was 20 μg/mL and 100 μg/mL for Carboplatin. Following 48 h of culture in 5% CO_2 at 37 °C, the wells were decanted and cells stained with 0.5% crystal violet in 20% methanol for 5 min at room temperature. Plates were washed eight times with tap water and dried at room temperature. The crystal violet was dissolved with 100 μL of 50% ethanol in 0.1 M sodium phosphate, and the absorbance measured at 570 nm with a spectrophotometer (Spectramax 250, Molecular Devices, Sunnyvale, CA).

In Vitro IRE Optimization

Effective *in vitro* IRE lethal electric field thresholds and pulse number effects were determined for optimal parameters to use in the combined method experiments, since these are the most common controllable pulse protocol parameters shown to alter effects on cell response and toxicity threshold. Aliquots (200 μL) of cell suspensions containing 2×10^6 cells/mL were placed into 4 mm gap electroporation cuvettes. A BTX generator (ECM830, Harvard Apparatus, Holliston, MA) delivered rectangular pulses at variable electric field strengths (0, 200, 400, 600, 800, and 1,600 V/cm) and pulse numbers (0–100, in increments of 10). Pulses were 50 μs long and delivered at a rate of 1 pulse per second. All treatments were performed in triplicate. Original parameter cytotoxicity was determined with crystal violet assay. Combined pulse with chemotherapeutic agent viability experiments were performed using luminescent cell viability assay.

Luminescent Cell Viability Assay

Five minutes following electric pulse delivery for IRE alone or IRE with drugs, cell suspensions were diluted to 1×10^4 cells/mL, and three 100 μL aliquots from each cuvette were plated into 96-well tissue culture plates. Plates were incubated for 24 h at 37 °C. Following equilibration to room temperature for 30 min, a luminescent cell viability assay was performed (Cell Titer Glo, Promega, Madison, WI) according to the manufacturer's instructions, followed by luminescence recording (LMax Luminometer, Molecular Devices, Sunnyvale, CA).

Hoechst 33342 Apoptosis Staining

In order to quantify the mechanisms causing cell death from the study, both cell lines were subjected to varying electric pulse strengths and drug concentrations for the same pulse parameters used in the viability study. Cells were pulsed in suspension as with previously outlined experiments. At 24 h after pulse delivery, a timeframe found adequate to visualize apoptotic effects, Hoechst 33342 staining was used to measure the fraction of apoptotic cells relative to controls. Aliquots from all treatments were diluted to 1×10^4 cells/mL and stained with 10 μM Hoechst 33342, and incubated for 1 h at 37 °C prior to examination *via* fluorescent microscopy (Leica DMRXA, Germany), with excitation centered at 360 nm and emission >425 nm. The percentage of apoptotic cells was determined from three independent quantifications, each counting ≥500 cells per treatment group, using image analysis software (NIS-Elements AR, Nikon, Japan) with a digital thresholding algorithm that labeled positively staining nuclei from the background of digital photomicrographs obtained with a 40× objective.

Transmission Electron Microscopy

Morphological cell changes as a function of electric fields alone and in combination with the drugs were visualized with transmission electron microscopy. At 24 h post-pulsing, cells were detached, washed, suspended in phosphate buffered solution, and concentrated by centrifugation at 250×*g* for 10 min. Cells were then fixed in 2.5% glutaraldehyde, post-fixed in 1% osmium tetroxide, dehydrated in ethanol, and embedded in plastic. Sections (50 nm) were obtained with an ultramicrotome, treated with lead citrate and uranyl acetate, and examined using a transmission electron microscope (Zeiss EMC-10 CA, Carl Zeiss SMT, Inc., Peabody, MA).

Statistical Analysis

One-way analysis of variance (ANOVA) was performed for pulse parameter optimization using commercial statistical software (SAS Version 9.1, Cary, NC). For the combined modality analyses, a two-way ANOVA was used for IRE with ECT experiments to determine the significance of interaction between the presence of electric field and drugs overall, as well as at specific dose combinations, which were compared to controls and either modality alone. Finally, a one-sided student's *t*-test was used to determine the presence of a statistically significant synergistic effect at various treatment combinations. This was used to evaluate whether the combined modality toxicity is greater than what would be expected when predicting the additive cytotoxicity sum from the individual modalities. The *t*-test compared the experimental cell viability (CV_e) for a given electric field, E, and drug dose, D, with a theoretical viability based on the additive combined effects of the two treatments. Theoretical additive cell viability (CV_t) was calculated for a given cell and drug protocol according to:

$$CV_t(E, D) = CV_0 - [CV_0 - CV_E(E, 0)] - [CV_0 - CV_D(0, D)] \quad (1)$$

where CV_t is the theoretical cell viability at a particular electric field and drug dose, while CV_0 is the control viability, CV_E is the viability for the electric pulse alone, and CV_D is the viability from the drug alone. This value was used to test the hypothesis that CV_e is less than the expected cell viability based on the difference from controls for the two modalities.

Numerical Models

Electric pulse effects can be correlated with the electric field distribution, which can be calculated using numerical modeling to predict treatment outcomes.[21] We employed this to determine the potential expanded therapeutic margins from a persistent ECT effect at sub-lethal electric fields from a typical IRE pulse protocol using Comsol Multiphysics 3.5a finite element modeling software (Comsol, Stockholm, Sweden). The effective IRE and enhanced pharmacotherapy electric field thresholds from the *in vitro* experiments were used to calculate predicted treatment margins for both therapeutic regimes. The physical setup of the model is depicted in the results section, where Mimics 14.0 and 3-matic 5.1 software (Materialise, Leuven, Belgium) were used to generate an image-derived volumetric mesh from a canine brain MRI of dimensions 7.5 × 5.0 × 4.8 cm. The model simulates two single-pole electrodes, each 1 mm in diameter, separated by 0.5 cm (center-to-center) with a 0.5 cm exposed tip and the rest of the length simulated as electrical insulation. Both electrode tips are set 0.5 cm into the brain. The electric field distribution is calculated by solving the governing equation:

$$\nabla \cdot (\sigma \nabla \phi) = 0 \quad (2)$$

where σ is the electric conductivity (S/m) of the tissue and ϕ is the electric potential (V). Due to the low conductivity of bone, the skull boundary of the brain was treated as electrical insulation. One of the electrodes was energized at V_0, and the other set to ground.

Two sets of numerical models were solved, one using a constant (static) baseline grey matter conductivity of $\sigma_0 = 0.285$ S/m,[7] and one that accounted for electroporation based conductivity changes in tissue due to effective cell membrane dielectric breakdown, giving conductivity as a function of electric field, $\sigma(E)$ (dynamic) based on the work described in Neal *et al.*[26] using the equation:

$$\sigma(E) = \sigma_0 + (\sigma_{max} - \sigma_0) \cdot \exp[-A \cdot \exp(-B \cdot E)] \quad (3)$$

where σ_0 and σ_{max} are the minimum and plateau conductivities within a single pulse, and A and B are unitless coefficients that vary with pulse length, t (s). This function was fit using curve parameters for a 50 μs long pulse, where $A = 3.053$ and $B = 0.00233$;[26] and a σ_{max} of 0.7791 S/m, based on the possible β-dispersion technique[9,26] using grey matter conductivity at 500 MHz.[10]

The numerical model simulated the electric field distribution within the tissue for the electrode setup solved for V_0 in 500 V increments between 500 and 2,500 V with static and dynamic conductivities. *In vitro* experimental results were used to predict effective electric field thresholds for the realm of complete IRE ablation. In addition, a threshold for enhancement from the inclusion of chemotherapeutics

was determined based on a degree of at least 50% increase in cytotoxicity from drug inclusion relative to pulses alone. Due to the complexity in calculating and administering chemotherapeutic biodistribution, the effective realm of enhancement assumes accurate and homogeneous drug concentration. For each model solution, the volumes of IRE and enhanced pharmacotherapy were numerically integrated to determine the potential selectively expanded therapeutic margins to kill infiltrative cells beyond the visible tumor.

RESULTS

Cellular Response Characterization

IRE Pulse Parameter Optimization

To investigate cytotoxicity from electric pulses alone, varying electric field pulses were used in a series of 90 pulses, each 50 μs long; typical IRE parameters for normal and neoplastic brain tissue.[12] There was no significant difference between the cell lines for the 50 or 90% effective dose electric fields (Figs. 1a and 1c). As a result, 800 V/cm was chosen for the pulse number experiments, where 90% cytotoxicity is observed below 80 pulses for J3T cells and 90 pulses for the U-87 MGs (Figs. 1b and 1d). In addition, the remaining combined IRE with ECT experiments used 80 and 90 total pulses for J3T and U-87 MG cells, respectively.

Chemotherapeutic Agent Cell Growth Inhibition

Chemotherapeutic response curves are presented in Fig. 2. To offer a general sense of inherent variability between cell line and drug susceptibility to the two drugs examined, function fits of the data provide mean ED50 values. The ED50 for Bleomycin was 136 ng/mL and 345 μg/mL for the J3T and U-87 MG lines, respectively, while the function fit-derived ED50s for Carboplatin were 687 ng/mL for J3T and 459 μg/mL for U-87 MG cells. Based on these values interpolated from the data, the ED50 concentrations for Carboplatin were higher than Bleomycin, while J3T showed greater susceptibility to both drugs. However, due to the wide range and low resolution of drug concentrations investigated, ED50 values were determined from function fits for general drug-only growth inhibition. The experimental two order of magnitude range between concentrations at ED50 suggests a higher resolution of experimental doses in this range should be used to more accurately determine ED50 values if required for other study purposes.

IRE Enhanced Pharmacotherapy Induced Glioma Cytotoxicity

The combination of electric pulses with varying chemotherapeutic drug concentrations was examined to determine the presence of a synergistic effect. For J3T cells, IRE combined with chemotherapeutic cytotoxicities were significantly greater (all $p < 0.01$) than for IRE or drug therapy alone over the entire ranges tested for both Bleomycin and Carboplatin (Figs. 2a and 2c) at electric fields of 200, 400, and 600 V/cm. For both drugs, there was significant negative association between viability and increasing drug dose at electric fields from 200 to 600 V/cm (all $p < 0.02$). At higher electric fields (800 and 1,600 V/cm), significant ($p < 0.04$) but mild increases in cytotoxic effect of IRE with ECT were noted only for Bleomycin or Carboplatin doses ≥1 μg/mL.

For U-87 MG cells at electric field strengths of 200–600 V/cm, the most significant ($p < 0.01$) cytotoxic effects of Bleomycin with IRE occurred only at the highest drug concentration tested (1 mg/mL, Fig. 2b). At electric field strengths ≥800 V/cm, there were mild cytotoxic effects of Bleomycin with IRE at concentrations ≥100 pg/mL ($p < 0.03$; Fig. 2b). Overall, there was more modest cytotoxic enhancement, most evident at higher doses for Carboplatin with IRE on U-87 MG than from Bleomycin (Figs. 2b and 2d). Compared to Carboplatin alone, progressively higher field strengths above 200 V/cm showed significantly ($p < 0.02$) enhanced U-87 MG cytotoxicity with successively lower Carboplatin doses (Fig. 2d). It is noted that transitioning from the crystal violet cell viability assay in the experiments from Fig. 1 (baseline pulse parameter experiments) to the luminescent cell viability assay used to generate the data for Fig. 2 (experimentally characterizing the interaction of pulses with drugs) resulted in a change to the experimental pulse strength for U87 cells required to reach <10% viability from electric field alone, although the J3T cell viability remains below 10% at 800 V/cm for both experimental approaches.

Overall, J3T glioma cells experience a significant degree of enhanced cytotoxicity by combining the IRE electric pulses with either drug, while the U87s have a more subtle response to the combined effect. Two-way ANOVA for J3T cells with the drugs and electric fields overall gives a statistically significant interaction ($p \ll 0.001$), suggesting the possibility of combined enhancement. Furthermore, Table 1 provides the results of two-way ANOVA and one-sided t-test with unequal variance for J3T cells at several electric fields and drug doses.

From this table, it can be seen that there is a significant degree of synergistic behavior at the 400 and

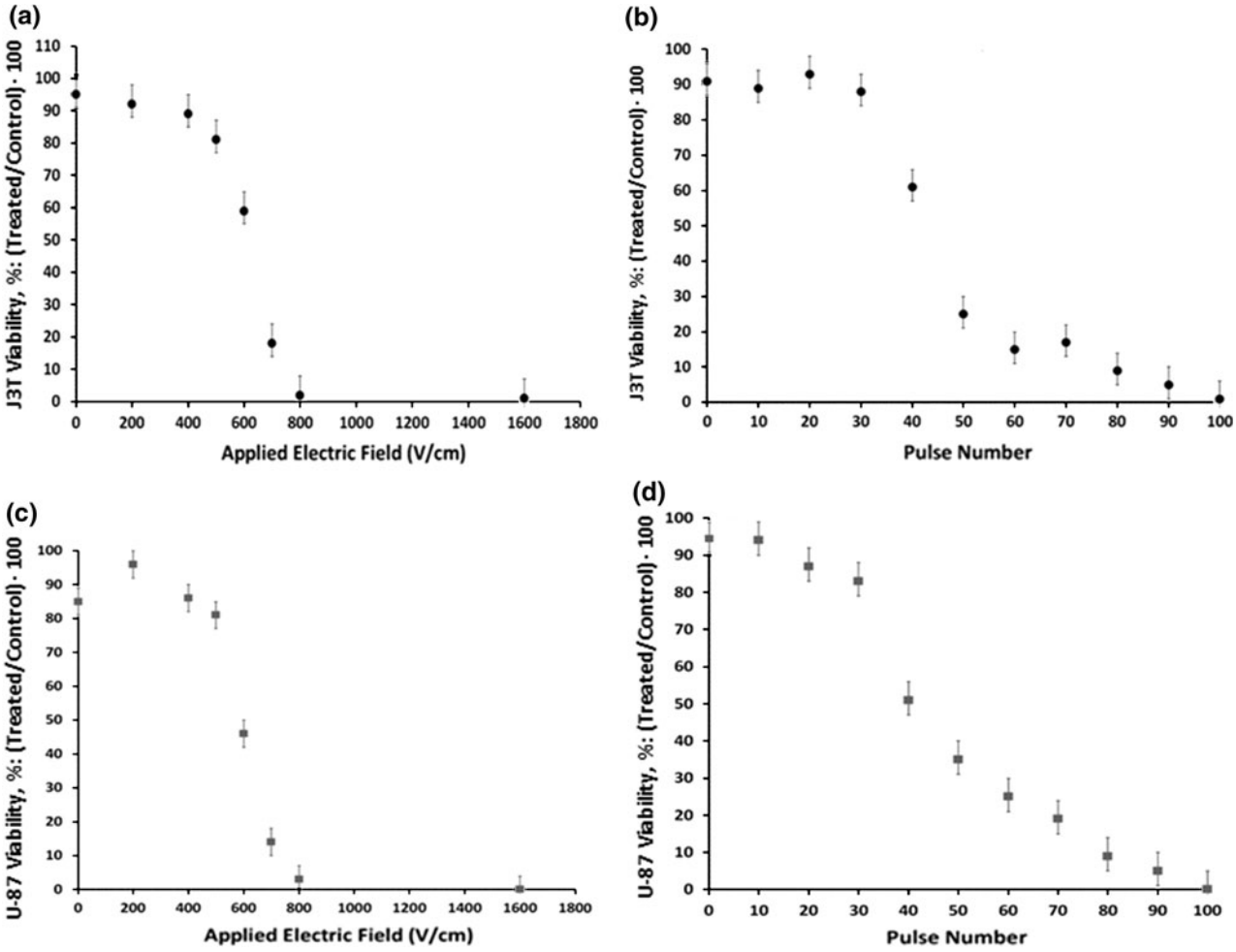

FIGURE 1. ***In vitro*** **electric pulse-only parameter results. (a, b) J3T and (c, d) U-87 MG cell viability as a function of (a, c) applied electric field for 90, 50 μs long pulses and (b, d) number of pulses using 50 μs pulses at 800 V/cm. All pulses delivered at 1 pulse per second.**

200 V/cm trials and lower drug doses, whereas by 600 V/cm, the pulses alone reduce the cellular viability beyond an extent where the combined effect of drug inclusion can be observed to make a significant difference. Similar states of statistical significance from both analyses occur for the J3T cells with both drugs, including the 200 V/cm trials with Carboplatin (not shown), suggesting that both drugs are suitable to attain the enhancement effect. The greatest presence of statistically significant enhancement at 200 and 400 V/cm is likely due to low extent of cytotoxicity from the pulses at these electric fields alone. These results indicate that the IRE electric pulses performed in conjunction with the drugs produces a synergistic enhancement effect that achieves greater cytotoxicity than the additive effects from either modality alone.

Based on the results from Fig. 2 and Table 1, the parameters to use in the numerical model were selected based on the J3T results in Fig. 2, and are noted to be cell-specific, as they may change with different patient glioma varieties.

IRE with ECT Induced Apoptosis of Glioma Cells

Although not the sole cell death mechanism, evidence of apoptosis was observed in response to all treatments by 24 h after pulsing. Morphologically (Fig. 3), apoptotic J3Ts and U-87 MGs displayed cellular shrinkage, cytoplasmic process loss and fragmentation (black arrows), formation of cytoplasmic apoptotic bodies (white arrowheads), and chromatin condensation (white arrows). Apoptotic IRE with ECT enhancement on J3Ts and U-87 MGs increased with higher drug concentrations and electric fields ≥400 V/cm (Fig. 4). This suggests that apoptosis plays a role as a cell death mechanism in addition to the cellular necrosis commonly noted for IRE.[8] Because apoptosis as a fractional death mechanism increases

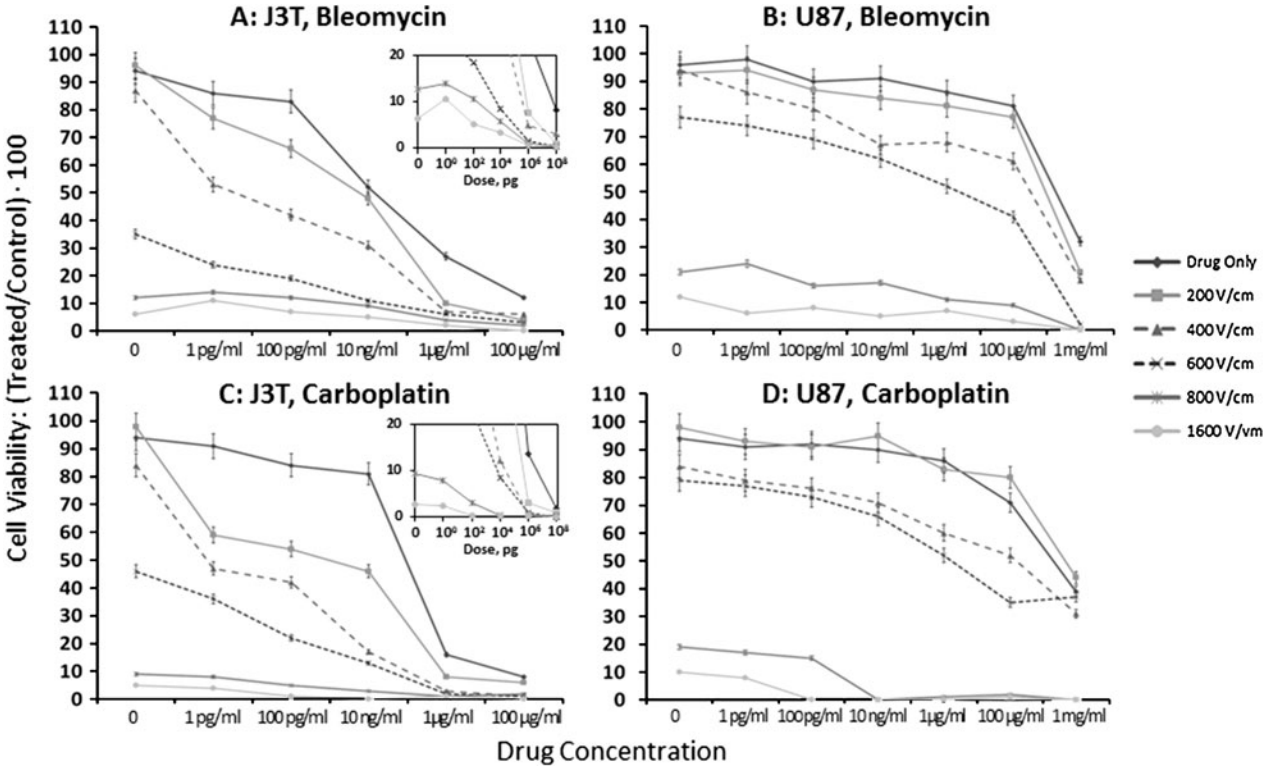

FIGURE 2. Overall IRE and Bleomycin or Carboplatin with IRE cytotoxicity. (a, c) J3T and (b, d) U-87 MG glioma cell viability at various pulse strengths and drug doses using 80 (J3T) and 90 (U-87 MG) pulses, each 50 μs long, at 1 pulse per second. $n = 3$ per group protocol.

TABLE 1. Selected statistical analysis for interaction and combinatorial effect for J3T cells.

Drug	Electric Field (V/cm)	Drug dose	Experimental viability* (%)	Theoretical viability* (%)	Two-way ANOVA significance	*t*-test for synergistic significance
BLM	200	1 pg	76 ± 5	85 ± 3	+++	−
BLM	200	100 pg	64 ± 2	81 ± 3	++	+++
BLM	200	10 ng	45 ± 5	50 ± 3	−	−
BLM	200	1 μg	8 ± 2	25 ± 3	+	+++
BLM	200	100 μg	1 ± 1	10 ± 2	++	++
BLM	400	1 pg	53 ± 3	73 ± 4	+++	+++
BLM	400	100 pg	40 ± 4	74 ± 3	+++	+++
BLM	400	10 ng	29 ± 3	43 ± 4	++	++
BLM	400	1 μg	5 ± 1	18 ± 3	++	+
BLM	400	100 μg	3 ± 1	3 ± 1	−	−
BLM	600	1 pg	24 ± 5	27 ± 4	−	−
CBP	400	1 pg	45 ± 3	80 ± 2	+++	+++
CBP	400	100 pg	40 ± 3	72 ± 3	+++	+++
CBP	400	10 ng	12 ± 2	67 ± 3	+++	+++
CBP	400	1 μg	0.7 ± 0.6	4 ± 3	−	−

BLM Bleomycin, *CBP* Carboplatin.
+++ $p < 0.001$, ++ $p < 0.01$,+ $p < 0.05$, − not significant.
* Values given as mean ± SD.

with higher drug doses at all electric fields, it suggests that apoptosis from IRE pulses combined with the drugs is also a pathway in which this combination achieves cell death.

Numerical Models

The numerical model (Fig. 5) was solved for the electric field distribution for the static and dynamic conductivity conditions, (Figs. 5c and 5d,

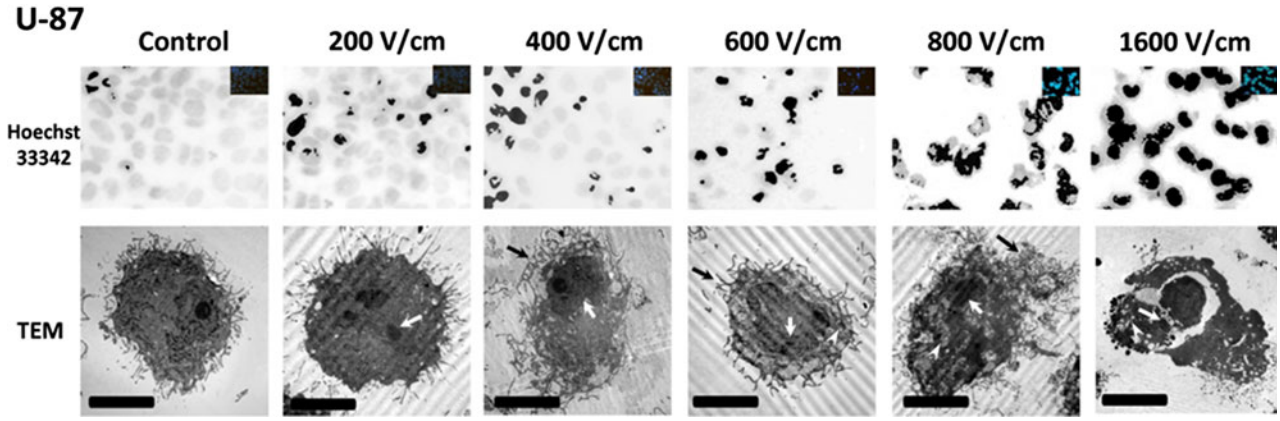

FIGURE 3. Apoptosis in U-87 MG glioma from IRE pulses alone. *Top panels* Apoptotic cells in Hoechst 33342 preparations (*inset*). *Bottom panels* Single cell glioma ultrastructural morphology in response to the applied electric fields, where presence of cytoplasmic process loss and fragmentation (*black arrows*), cytoplasmic apoptotic bodies (*white arrowheads*), and chromatin condensation (*white arrows*) are evident. (*TEM* transmission electron microscopy, *bar* 2 μm in all panels).

respectively). Applying the results from the *in vitro* experiments, electric field thresholds of 400 and 800 V/cm were selected to represent the regions of tissue experiencing enhanced drug cytotoxicity and IRE, respectively. These volumes were integrated for the results from both conductivity distributions for the applied voltages from 500 to 2,500 V/cm. This is because the J3T cells reach $<10\%$ viability from pulses alone at 800 V/cm, while the inclusion of 1 ng/mL of either drug with 400 V/cm pulses results in a cytotoxicity increase of over 50%.

Tissue volumes experiencing IRE and electric pulse mediated increased chemotherapeutic cytotoxicity were numerically integrated within the brain to quantify increased treatment volume when incorporating enhanced drug uptake (Table 2). The dynamic conductivity function consistently resulted in larger volumes for all voltages at both electric field thresholds. Volume factor increases were calculated as volume at 400 V/cm divided by volume at 800 V/cm. Predicted affected volumes were shown to increase between 2.05 and 3.20 times over the entire range of models examined, with greater increases found at lower applied voltages.

DISCUSSION

From the numerical simulations, combinatorial IRE with ECT increases the therapeutic volume by 2.1–3.2 times compared to IRE alone. This increase in volume may permit selectively expanding therapeutic margins beyond the IRE targeted, visible tumor margin. The potential for improving IRE therapy with adjuvant chemotherapeutics is consistent with other ablation therapies that show improved treatment outcomes from multi-modality approaches.[30]

The results presented in Table 1 indicate that the enhanced cytotoxicity observed in the *in vitro* experiments combining IRE pulse protocols with the drugs is a result of a synergistic enhancement, where the combination achieves greater cell death through cooperating both mechanisms in unison than the additive cytotoxicities of each modality alone. Because the greatest degree of combined enhancement occurs at the lower drug doses and electric fields, it is likely that the synergistic effect is a result of drugs getting into the cells due to improved intracellular macromolecule transport via electroporation rather than requiring sufficiently high doses for the drugs to naturally enter the cells with intact membranes. This further suggests that the enhanced mechanism is a result of high intrinsic cytotoxicity but poor permeability of the drugs used in this study.

The electric field thresholds used in the model were based on the J3T results, with 800 V/cm as the IRE threshold, which resulted in $<10\%$ viability from the pulses alone; while the same pulse protocol produced $>50\%$ drops in cellular viability at 10 ng/mL of either drug at 400 V/cm. The $>50\%$ drop in this realm makes 400 V/cm a potential selective agent to destroy many infiltrative cancer cells beyond the tumor margin while keeping doses low enough to avoid killing unacceptable levels of healthy cells from the drug alone. Although this combinatorial effect would ideally kill 100% of the infiltrative cells beyond the tumor margin, the issues that would result from also killing such a large volume of healthy neural tissue with IRE or very high drug concentrations make the combinatorial effect and $>50\%$ increase in cytotoxicity preferable in certain glioma cases. There was less significant enhancement for these parameters with the U87 cells, suggesting variable response to this

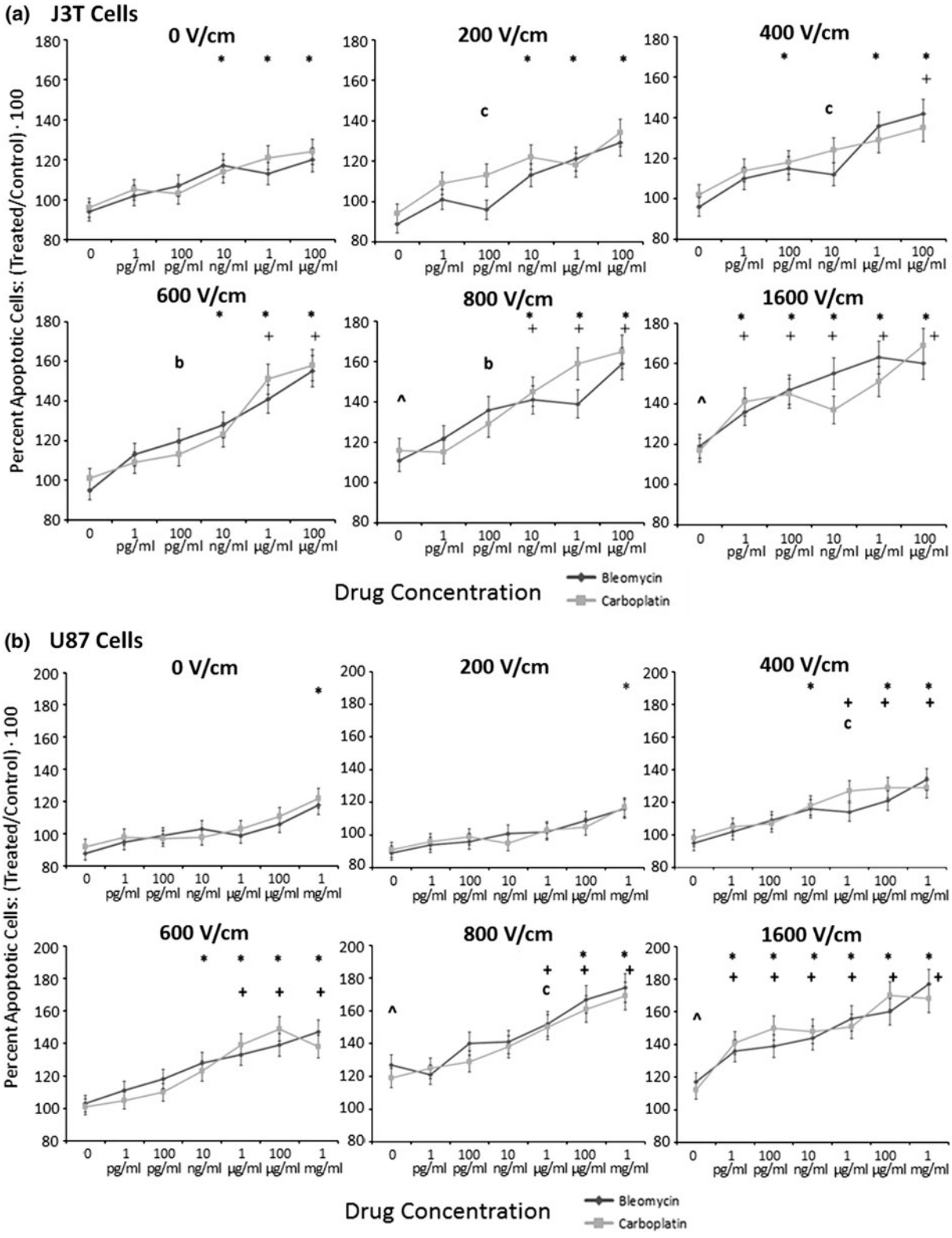

FIGURE 4. Apoptosis for IRE and IRE with ECT. Observed for (a) J3T and (b) U-87 MG glioma as determined from Hoechst 33342 staining. $n = 3$ per group protocol * Bleomycin and Carboplatin with IRE significantly ($p < 0.05$) different than IRE alone (drug concentration zero). *b* Bleomycin with IRE significantly different ($p < 0.05$) than IRE alone *c* Carboplatin with IRE significantly different ($p < 0.05$) than IRE alone ^ IRE induced apoptosis significantly different ($p < 0.05$) than untreated control + apoptosis with IRE and Bleomycin or Carboplatin significantly different ($p < 0.05$) than drug therapy alone.

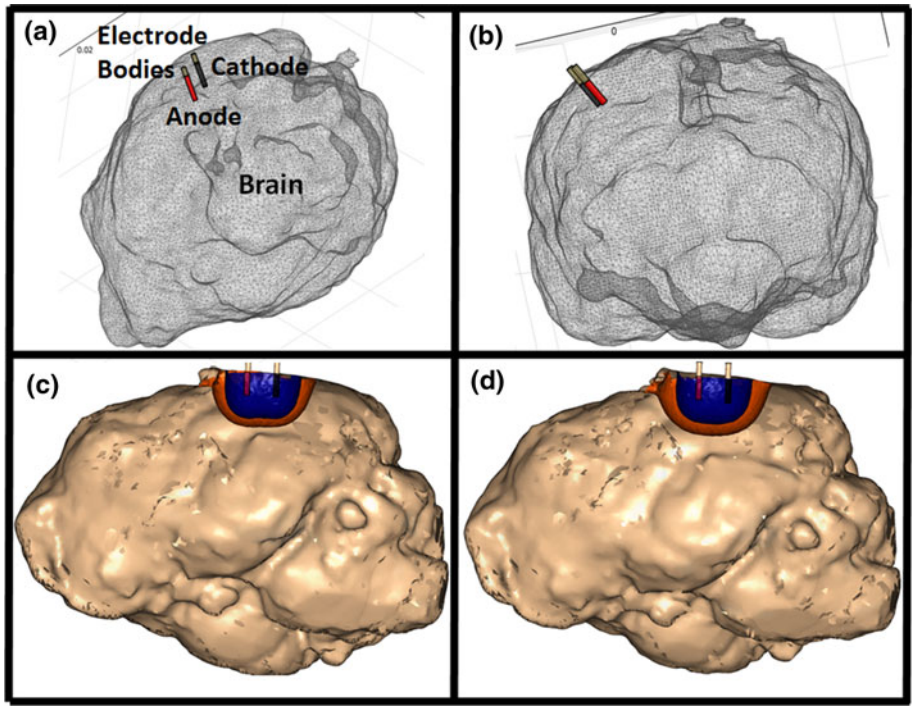

FIGURE 5. Numerical model of electric field distribution. (a, b) model setup showing canine brain volumetric mesh from (a) above isometric and (b) front views. (c, d) model solution at 2,500 V applied voltage depicting volumes experiencing IRE (*blue*, 800 V/cm) and ECT (*red*, 400 V/cm) using c constant and d dynamic conductivity techniques (*side view*).

TABLE 2. Increase in numerical model treatment volume by including 400 V/cm ECT regime.

Model	Applied voltage (V)	Volume at 800 V/cm (cm^3)	Volume at 400 V/cm (cm^3)	Volume increase factor (x)
Static	500	0.0760	0.218	2.87
	1,000	0.218	0.471	2.16
	1,500	0.346	0.716	2.07
	2,000	0.471	0.964	2.05
	2,500	0.593	1.22	2.06
Dynamic	500	0.0813	0.260	3.20
	1,000	0.237	0.601	2.54
	1,500	0.385	0.950	2.47
	2,000	0.532	1.30	2.45
	2,500	0.676	1.67	2.47

approach depending on tumor type, where IRE with ECT may be better suited for some tumors than others.

Where IRE has a very sharp *in vivo* delineation from entirely dead cells within ablation zones to regions of no death, it is ideally suited for killing the entirety of the visible tumor. However, because IRE treatments require muscular blockades to mitigate muscular contraction from electroporation therapy pulses, procedures also require general anesthesia. This eliminates the possibility for immediately determining the effects of brain tissue ablation on its functionality, as is possible with "awake brain surgery" tumor removal procedures.[39] IRE therefore, is not an ideal candidate to iteratively expand treatment margins progressively beyond visible tumor while intraprocedurally evaluating deficits in cognitive function. Preservation of brain function is a premium in glioma treatments. Therefore, utilizing the enhancement to target this region and destroy as many cancerous cells as possible should be significant in attaining working treatments and prolonging patient length and quality of life, and is at the least an important step in approaching working cures that can destroy all cancerous cells from a brain tumor.

The numerical model in this study investigated applied voltages from 500 up to 2,500 V. The separation distance used in this model resulted in voltage-to-distance ratios as high as 5,000 V/cm. The high applied voltages were included to ensure consistency in the

trend of treatment volume increase when including the 400 V/cm persistent ECT regime. This effect should be maintained for different physical electrode geometries and tissues.

The numerical model showed an increased treatment margin of approximately 0.5 cm for the 2,500 V case based on dynamic tissue properties using the β-dispersion characteristics of brain tissue as suggested in Neal *et al.*[26], though future work should confirm these parameters. Although this is short of the desired 2 cm for MG treatment, it remains significant. It should be noted that the electric field thresholds were derived from *in vitro* experiments, while evidence suggests electroporation effect thresholds may change *in vivo*. For instance, while 800 V/cm was selected as an IRE threshold based on the *in vitro* MG cell lines, an IRE threshold of 500 V/cm was found in healthy canine brain.[12] There will also be differences between healthy and cancerous tissue.

IRE with ECT-induced apoptosis was evaluated at 24 h. Eliminating this time constraint *in vivo* would enable observation of slower developing apoptotic processes than were evident in this study. Finally, electroporation increases vascular permeability, with noted edema in electroporated tissues.[19,35] This disrupts the BBB at irreversibly and reversibly electroporated regions, as recently shown in MRI,[13,16] and has been known to improve selective drug biotransport into the targeted region.[34] Therefore, it is likely that additional combinatorial IRE with ECT benefits will be appreciated for various tumors *in vivo* due to secondary effects of improved localization for chemotherapeutic regimens in the targeted region.

Another important note for this study regards the drug dose used *in vitro* vs. the *in vivo* implications. The experimental *in vitro* drug doses were selected to estimate the maximum combinatorial effect on apoptosis and overall cell death. Direct translation of these doses to *in vivo* scenarios is difficult due to the increased complexity of chemotherapeutic biodistribution for *in vivo* systems, including considerations regarding blood perfusion, passive drug accumulation at tumor sites, and renal drug clearance. Additionally, direct *in vivo* dose comparisons are further complicated by the edematic and vascular occlusion effects from electroporation and ECT.[8,18,35] Finally, *in vivo* systems utilizing the combined regions of cell death may get significantly larger treatment zones than from either modality alone, increasing the risk for post-ablation syndrome. However, the literature has not indicated this issue thus far when using IRE to ablate large volumes of patient tumors.[37]

Although an increased degree of cytotoxicity was found when incorporating the chemotherapeutics in addition to the IRE-relevant electric pulses; the cell death increase at the 400 V/cm threshold was insufficient to ensure complete destruction of all tumor cells beyond the 800 V/cm IRE threshold. While the increased cytotoxicity will still likely benefit patient outcomes, future work should examine the technical challenges in optimizing the maximum benefit from the enhanced chemotherapeutic uptake while still confirming complete targeted region ablation. Such approaches may include novel electric pulse shapes to encourage electrokinetic movement of the chemicals into the cells following electroporation, or distinct sets of pulses that target each modality separately. However, the objective of this preliminary study was to examine the potential enhancement from the simplest-case scenario, in which low ECT drug doses are administered immediately prior to performing a standard IRE procedure, where it is suggested from the *in vitro* evidence that there should be some benefit.

CONCLUSIONS

This study supports a benefit for combining IRE focal ablation with adjuvant chemotherapy for the treatment of MGs. IRE electric pulses shown to produce focal ablations in brain were employed with *in vitro* experiments to realize a regime of sub-lethal electric fields capable of enhancing chemotherapeutic toxicity. This was shown to occur even when using higher pulse numbers common in clinical IRE protocols. Imaging showed that apoptosis plays an important role in the cell death mechanisms resulting from the combinatorial treatment. Numerical models used the data from the *in vitro* experiments, and predict the effective treatment volumes will more than double using the combined modality approach in all simulated scenarios. These preliminary results support future investigations into IRE with ECT for *in vivo* combinatorial treatment, particularly of glioma.

ACKNOWLEDGMENTS

This work was supported by the Coulter Foundation, NSF CAREER Award CBET-1055913, and Whitaker International Scholars Program. The authors thank Kathy Lowe for assistance with cell morphology and histology work.

CONFLICT OF INTEREST

REN, JHR, PAG, RVD, JLR: Patent holders of "Irreversible Electroporation to Treat Aberrant Masses," and have pending patents in the area of

irreversible electroporation in general, but which does not directly relate to the content submitted here. RVD provides minimal consulting and has received research funding in the area of numerical modeling of electric fields. This manuscript has not been previously published, in whole or in part, nor is it concurrently under consideration elsewhere.

REFERENCES

[1]Agerholm-Larsen, B., H. K. Iversen, P. Ibsen, J. M. Moller, F. Mahmood, *et al*. Preclinical validation of electrochemotherapy as an effective treatment for brain tumors. *Cancer Res*. 71:3753–3762, 2011.

[2]Ahmed, M., C. L. Brace, F. T. Lee, and S. N. Goldberg. Principles of and advances in percutaneous ablation. *Radiology* 258:351–369, 2011.

[3]Al-Sakere, B., F. Andre, C. Bernat, E. Connault, P. Opolon, *et al*. Tumor ablation with irreversible electroporation. *PLoS One* 2:e1135, 2007.

[4]Au, J. T., J. Wong, A. Mittra, S. Carpenter, D. Haddad, *et al*. Irreversible electroporation is a surgical ablation technique that enhances gene transfer. *Surgery* 150:474–479, 2011.

[5]Cheung, W., H. Kavnoudias, S. Roberts, B. Szkandera, W. Kemp, *et al*. Irreversible electroporation for unresectable hepatocellular carcinoma: initial experience and review of safety and outcomes. *Technol. Cancer Res. Treat*. 12:233–241, 2013.

[6]Davalos, R., L. Mir, and B. Rubinsky. Tissue ablation with irreversible electroporation. *Ann. Biomed. Eng*. 33:223–231, 2005.

[7]Duck, F. A. Physical properties of tissue: a comprehensive reference book. New York: Academic Press, 1990.

[8]Edd, J. F., L. Horowitz, R. V. Davalos, L. M. Mir, and B. Rubinsky. *In vivo* results of a new focal tissue ablation technique: irreversible electroporation. *IEEE Trans. Biomed. Eng*. 53:1409–1415, 2006.

[9]Foster, K. R., and H. P. Schwan. Dielectric properties of tissues and biological materials: a critical review. *Crit. Rev. Biomed. Eng*. 17:25–104, 1989.

[10]Gabriel, S., R. W. Lau, and C. Gabriel. The dielectric properties of biological tissues: II. Measurements in the frequency range 10 Hz to 20 GHz. *Phys. Med. Biol*. 41:2251–2269, 1996.

[11]Garcia, P. A., T. Pancotto, J. H. Rossmeisl, Jr., N. Henao-Guerrero, N. R. Gustafson, *et al*. Non-thermal irreversible electroporation (N-TIRE) and adjuvant fractionated radiotherapeutic multimodal therapy for intracranial malignant glioma in a canine patient. *Technol. Cancer Res. Treat*. 10:73–83, 2011.

[12]Garcia, P., J. Rossmeisl, R. Neal, T. Ellis, J. Olson, *et al*. Intracranial nonthermal irreversible electroporation: *in vivo* analysis. *J. Membr. Biol*. 236:127–136, 2010.

[13]Garcia, P. A., J. H. Rossmeisl, Jr., J. L. Robertson, J. D. Olson, A. J. Johnson, *et al*. 7.0-T magnetic resonance imaging characterization of acute blood–brain-barrier disruption achieved with intracranial irreversible electroporation. *PLoS ONE* 7:e50482, 2012.

[14]Garrido, W., M. Munoz, R. San Martin, and C. Quezada. FK506 confers chemosensitivity to anticancer drugs in glioblastoma multiforme cells by decreasing the expression of the multiple resistance-associated protein-1. *Biochem. Biophys. Res. Commun*. 411:62–68, 2011.

[15]Heller, R., M. J. Jaroszeski, D. S. Reintgen, C. A. Puleo, R. C. DeConti, *et al*. Treatment of cutaneous and subcutaneous tumors with electrochemotherapy using intralesional bleomycin. *Cancer* 83:148–157, 1998.

[16]Hjouj, M., D. Last, D. Guez, D. Daniels, S. Sharabi, *et al*. MRI study on reversible and irreversible electroporation induced blood–brain barrier disruption. *PLoS ONE* 7:e42817, 2012.

[17]Hochberg, F. H., and A. Pruitt. Assumptions in the radiotherapy of glioblastoma. *Neurology* 30:907–911, 1980.

[18]Jarm, T., M. Cemazar, D. Miklavcic, and G. Sersa. Antivascular effects of electrochemotherapy: implications in treatment of bleeding metastases. *Expert Rev. Anticancer Ther*. 10:729–746, 2010.

[19]Lee, E. W., C. T. Loh, and S. T. Kee. Imaging guided percutaneous irreversible electroporation: ultrasound and immunohistological correlation. *Technol. Cancer Res. Treat*. 6:287–293, 2007.

[20]Linnert, M., and J. Gehl. Bleomycin treatment of brain tumors: an evaluation. *Anticancer Drugs* 20:157–164, 2009.

[21]Miklavcic, D., D. Semrov, H. Mekid, and L. M. Mir. A validated model of *in vivo* electric field distribution in tissues for electrochemotherapy and for DNA electrotransfer for gene therapy. *Biochimica et Biophysica Acta* 1523:73–83, 2000.

[22]Miklavcic, D., D. Semrov, H. Mekid, and L. M. Mir. A validated model of *in vivo* electric field distribution in tissues for electrochemotherapy and for DNA electrotransfer for gene therapy. *Biochim Biophys Acta* 1523:73–83, 2000.

[23]Mir, L. M., and S. Orlowski. Mechanisms of electrochemotherapy. *Adv. Drug Deliv. Rev*. 35:107–118, 1999.

[24]Mirimanoff, R. O., T. Gorlia, W. Mason, M. J. Van den Bent, R. D. Kortmann, *et al*. Radiotherapy and temozolomide for newly diagnosed glioblastoma: recursive partitioning analysis of the EORTC 26981/22981-NCIC CE3 phase III randomized trial. *J. Clin. Oncol*. 24:2563–2569, 2006.

[25]Neal, II, R. E., W. Cheung, H. Kavnoudias, and K. R. Thomson. Spectrum of imaging and characteristics for liver tumors treated with irreversible electroporation. *J. Biomed. Sci. Eng*. 5:813–818, 2012.

[26]Neal, II, R. E., P. A. Garcia, J. L. Robertson, and R. V. Davalos. Experimental characterization and numerical modeling of tissue electrical conductivity during pulsed electric fields for irreversible electroporation treatment planning. *IEEE Trans. Biomed. Eng*. 59:1076–1085, 2012.

[27]Neal, II, R. E., J. H. Rossmeisl, Jr., P. A. Garcia, O. I. Lanz, N. Henao-Guerrero, *et al*. Successful treatment of a large soft tissue sarcoma with irreversible electroporation. *J. Clin. Oncol*. 29:e372–e377, 2011.

[28]Onik, G., P. Mikus, and B. Rubinsky. Irreversible electroporation: implications for prostate ablation. *Technol. Cancer Res. Treat*. 6:295–300, 2007.

[29]Prados, M. D., and V. Levin. Biology and treatment of malignant glioma. *Semin. Oncol*. 27:1–10, 2000.

[30]Qian, J., G. S. Feng, and T. Vogl. Combined interventional therapies of hepatocellular carcinoma. *World J. Gastroenterol*. 9:1885–1891, 2003.

[31]Roux, S., C. Bernat, B. Al-Sakere, F. Ghiringhelli, P. Opolon, *et al*. Tumor destruction using electrochemotherapy followed by CpG oligodeoxynucleotide injection induces distant tumor responses. *Cancer Immunol. Immunother*. 57:1291–1300, 2008.

[32]Rubinsky, J., G. Onik, P. Mikus, and B. Rubinsky. Optimal parameters for the destruction of prostate cancer using irreversible electroporation. *J. Urol*. 180:2668–2674, 2008.
[33]Sabel, M. S. Cryo-immunology: a review of the literature and proposed mechanisms for stimulatory versus suppressive immune responses. *Cryobiology* 58:1–11, 2009.
[34]Salford, L. G., B. R. Persson, A. Brun, C. P. Ceberg, P. C. Kongstad, *et al*. A new brain tumour therapy combining bleomycin with *in vivo* electropermeabilization. *Biochem. Biophys. Res. Commun*. 194:938–943, 1993.
[35]Sersa, G., T. Jarm, T. Kotnik, A. Coer, M. Podkrajsek, *et al*. Vascular disrupting action of electroporation and electrochemotherapy with bleomycin in murine sarcoma. *Br. J. Cancer*. 98:388–398, 2008.
[36]Sersa, G., D. Miklavcic, M. Cemazar, Z. Rudolf, G. Pucihar, *et al*. Electrochemotherapy in treatment of tumours. *Eur. J. Surg. Oncol*. 34:232–240, 2008.
[37]Thomson, K. R., W. Cheung, S. J. Ellis, D. Federman, H. Kavnoudias, *et al*. Investigation of the safety of irreversible electroporation in humans. *J. Vasc. Interv. Radiol*. 22:611–621, 2011.
[38]Venkatesan, A. M., B. J. Wood, and D. A. Gervais. Percutaneous ablation in the kidney. *Radiology* 261:375–391, 2011.
[39]Yordanova, Y. N., S. Moritz-Gasser, and H. Duffau. Awake surgery for WHO Grade II gliomas within "noneloquent" areas in the left dominant hemisphere: toward a "supratotal" resection. Clinical article. *J. Neurosurg*. 115:232–239, 2011.